



# Three-dimensional prospectivity modeling based on fuzzy logic and geometric average: a case study from Sansong district, Yongyu apatite deposit, DPR Korea

Yon-Ho Kim<sup>1</sup> · Kwang-U Choe<sup>1</sup>

Received: 23 February 2023 / Accepted: 25 February 2024 / Published online: 11 March 2024  
© Saudi Society for Geosciences and Springer Nature Switzerland AG 2024

## Abstract

In this paper, we applied two kinds of knowledge-driven methods, one using the fuzzy logic and another using geometric average to evaluate 3D mineral prospectivity for Sansong district, Yongyu apatite deposit, in the Phyongnam Basin, DPR Korea. Based on the ore geology studies of apatite deposits and the available spatial datasets in the study area, we used four independent evidential maps for 3D apatite deposit prospectivity modeling. They include (1) carbonatite, (2) biotite gneiss, (3) granitic gneiss, and (4)  $P_2O_5$  values from the borehole data. The evidential factors were modeled into 3D space, and 3D  $P_2O_5$  values from the borehole data were transformed into continuous values of the [0, 1] range using logistic sigmoid. In 3D MPM just as 2D MPM, it is very economic and efficient to simultaneously apply the fuzzy logic and geometric average methods for mineral prospectivity modeling of the study area because two predictive models can use the same fuzzification methodology based on fuzzy membership function. Our strategy is to fuzzify the evidential maps before applying the geometric average as well as in the fuzzy logic. The results for the two predictive models were validated by the prediction efficiency method. The results demonstrated that most of the validation data were distributed in voxels with high prospectivity values. Although the validation results were slightly worse than those in 2D MPM case study, our case studies suggested that both predictive models and their modeling results are useful for evaluating 3D prospectivity of apatite deposits in Sansong district, Yongyu apatite deposit, DPR Korea.

**Keywords** 3D prospectivity modeling · Yongyu deposit · Geometric average · Fuzzy logic · Prediction efficiency

## Introduction

The predictive models in GIS-based mineral prospectivity modeling (MPM) can be typically subdivided into two main categories: knowledge-driven and data-driven models. The main characteristics of data-driven methods are that they are based on the spatial relationship between known mineral occurrences and input evidential layers and they are commonly suitable for brown fields (well-explored regions). Although many sophisticated data-driven methods based on artificial intelligence have been reported (Xiong and Zuo 2018; Zhang et al. 2019; Li et al. 2020; Chen et al. 2020;

Prado et al. 2020; Shirazy et al. 2021; Deng et al. 2022), the weights of evidence (WofE) method remains one of the most widely used data-driven approaches, and many case studies and modified or hybrid versions for MPM have been reported (Ford et al. 2015; Kreuzer et al. 2015; Ren et al. 2016; Liu and Cheng 2019; Mao et al. 2019). In contrast, knowledge-driven approaches, unlike data-driven techniques, only depend on expert opinions, and they include fuzzy logic (Ford et al. 2015; Nykänen et al. 2015; Yousefi and Carranza 2015a; Tao et al. 2021; Behera and Panigrahi 2021), index overlay (Yousefi and Carranza 2015b; Li et al. 2022), Dempster-Shafer belief theory (Mohammadpour et al. 2021), analytical hierarchy process (Li et al. 2022; Shabani et al. 2022; Shirazi et al. 2022), and data envelopment analysis (Hosseini and Abedi 2015). Knowledge-driven methods are commonly applied in green fields (under-explored regions), and it is particularly suitable for the case studies in DPRK because most of MPM studies might be implemented in green fields rather than in brown fields.

Responsible Editor: Biswajeet Pradhan

✉ Yon-Ho Kim  
yh.kim@ryongnamsan.edu.kp

<sup>1</sup> Faculty of Geology, Kim Il Sung University, Pyongyang, Democratic People's Republic of Korea

The geometric average belongs to a category of knowledge-driven methods; therefore, it can be used in green fields, and it also has some inherent advantages over other methods (Yousefi and Carranza 2015c). The geometric average method can not only effectively treat some uncertainties during MPM but also it does not require the same unit for different evidential values. In addition, it is easy to implement because it is based on a relatively simple model. The fuzzy logic method is also a kind of knowledge-driven methods which can effectively capture the fuzzy nature of evidential maps used in MPM, and recent researches focus on hybrid methods of the fuzzy logic and other techniques such as WofE (Mao et al. 2019; Behera and Panigrahi 2021). In particular, data fusion techniques by the hybrid fuzzy-AHP have been recently used in the field of MPM (Khosravi et al. 2022; Shabani et al. 2022; Shirazi et al. 2022). Our hybrid strategy is to fuzzify the evidential maps before applying the geometric average model as well as in the fuzzy logic. Although our previous studies (Kim et al. 2019) have revealed that GIS modeling techniques based on geometric average and fuzzy logic models can provide a fast and economic way to separate prospectivity target areas for Cu polymetallic mineralization in the study area, we recognize that it is necessary to efficiently incorporate 3D predictive models within available 3D GIS and to test generalization ability of our methodology in different case studies. Furthermore, 3D MPM studies have been rarely reported until now and just initiated in recent years in DPRK even though it has been already the main research field in many other parts of the world (Li et al. 2016; Mao et al. 2019; Mohammadpour et al. 2021; Deng et al. 2022). It will be the first attempt to implement 3D prospectivity modeling of non-metal deposits in DPRK, and it has also a practical significance to separate some prospectivity target areas for future mining and production in Sansong district, Yongyu apatite deposit.

The aims of the paper are (1) to answer the question “How can we extend the fuzzy logic and the geometric average methods from 2 to 3D studies?”, (2) to separate target areas in the Sansong district of the Yongyu deposit to prepare new areas for future drilling and mining, and (3) to compare the results of 3D MPM for non-metal deposits with those of our previous 2D MPM for Cu polymetallic deposits. To do this, we implement 3D modeling for four factors extracted from the geological database in Sansong district, Yongyu apatite deposit, using SGrid object of commercial 3D GIS software (GOCAD), and they are integrated based on two predictive models—one using the fuzzy logic and another using the geometric average. We created two 3D prospectivity models in the study area, compared the results of two predictive models, and tested possibility of their application for 3D MPM of non-metal deposits by using prediction efficiency curve based on the validation data in the study area. We also compared our results with those in the previous 2D

study (Kim et al. 2019). In our study, we choose the Sansong district of the Yongyu apatite deposit as the research area to verify our method and to provide some new target areas for future mining and production. In the Yongyu deposit, the study area is considered to be the only choice for the future mining and production, and the urgent task is to separate some new prospectivity volumes to design more detailed geological survey and to drill some additional boreholes.

## Geological background

### General geology

Yongyu apatite deposit is situated in Yongyu district of Pyongwon county, South Pyongan Province, DPR Korea. The study area is tectonically located in the northwestern part of Phyongnam Basin (Fig. 1). The Phyongnam Basin borders Rangnim Massif by Chongchongang fault zone on the north and Kyonggi Massif by Wonsan-Seoul fault zone on the south. And it can be subdivided into Pyongyang uplift and Sariwon-Sohung Basin, and it also includes several emergences such as Yangdok Emergence, Pyongwon Emergence, Anak-Sinchon Emergence, and Ichon Emergence (Paek et al. 1993).

The study area tectonically belongs to Pyongwon Emergence, Pyongyang uplift of Phyongnam Basin. The geology of the study area basically consists of sedimentary metamorphic rocks, altered granites, and carbonate rocks of Paleoproterozoic strata, Jungsan Complex (Fig. 2).

In the study area, the sedimentary metamorphic rocks include biotite gneiss, garnet biotite gneiss, biotite schist, amphibole schist, and siliceous shale. The altered granites consist of gneissic biotite granitite, garnet biotite granitite, chlorite biotite granitite, and amphibole biotite granitite. And altered granites contain different amount of altered residues of biotite gneiss, siliceous schist, and metabasite. The carbonate rocks are included in the sedimentary metamorphic rocks and altered granites of Paleoproterozoic Jungsan Complex. In the study area, NW and NE trending fault systems are developed and NW trending faults are cut and transposed by NE trending faults. The area for current study was selected because of two practical reasons: (1) it is necessary to provide spatial information where to focus future drilling in further development for Sansong district, Yongyu apatite deposit, and (2) availability of borehole datasets.

### Ore geology

The apatite deposits in DPR Korea are divided into magmatic, carbonatite, sedimentary metamorphic pegmatic, skarn, and hydrothermal (Choe et al. 2011). The magmatic apatite deposits are genetically and spatially associated

**Fig. 1** Location of the study area with tectonic units (the black-red box indicates the location of the study area; TFB, Tumangang Fold Belt; KM, Kwanmo Massif; KMB, Kilju-Myongchon Basin; HRB, Hyesan-Riwon Basin; RM, Rangnim Massif; PB, Phyongnam Basin) (Paek et al. 1993)

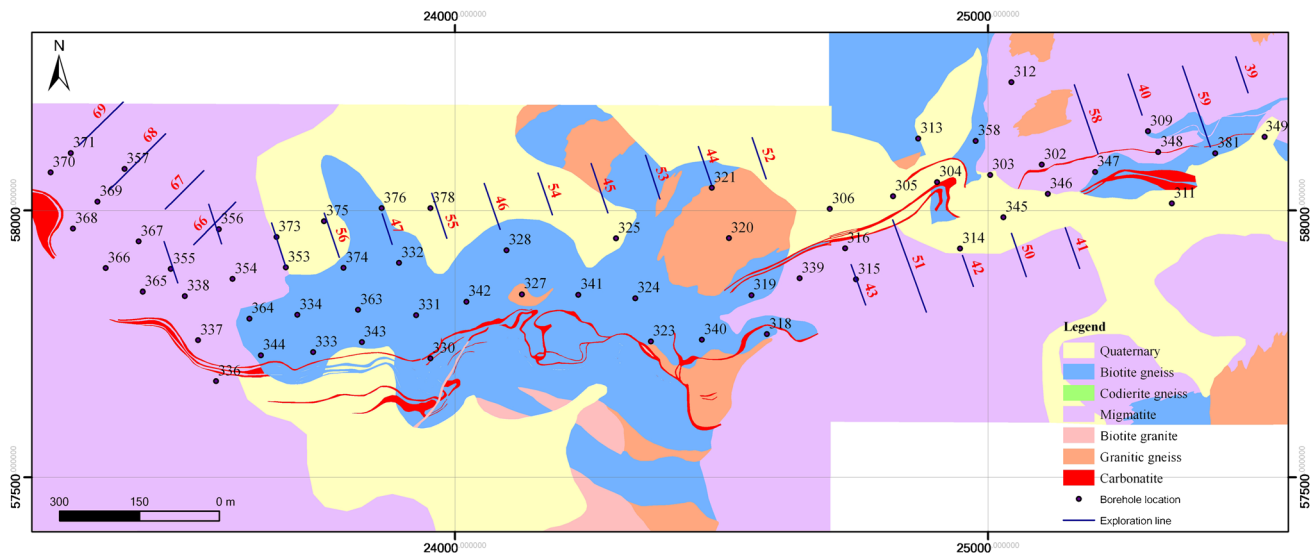
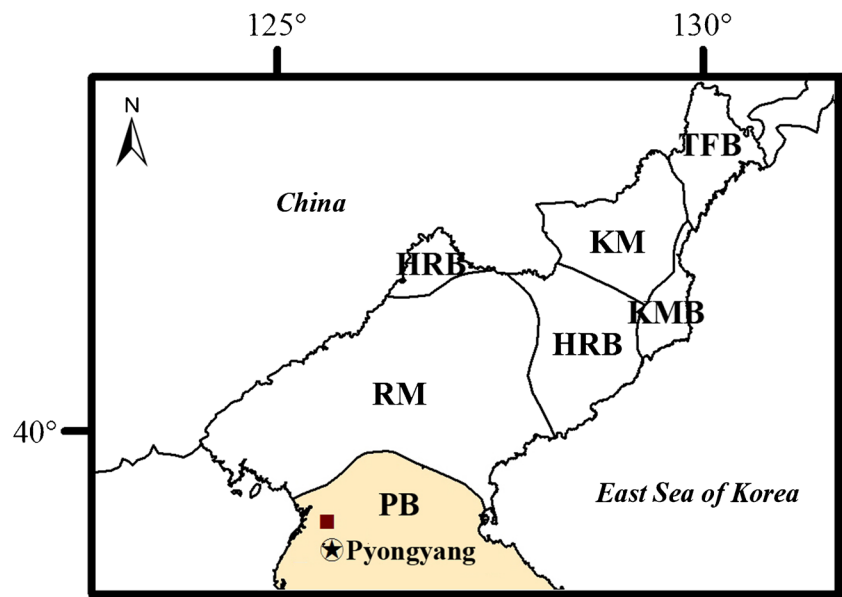


**Fig. 2** Geological map of the study area, exploration profiles, and borehole locations

with alkaline-mafic, alkaline-intermediate, and alkaline-ultramafic rocks within Andol Complex, Pyoksong Complex, Sakju Complex, Yonsan Complex, and Pyongyang Complex. The apatite ore bodies of this type deposit are mainly developed within the altered rocks formed by biotitization and chloritization from amphibole and pyroxene and albitization-zoisitization from plagioclase. Some deposits of this type might be included in the category of magmatic-metamorphic deposits. The majority of sedimentary apatite deposits are developed within the sedimentary rocks of Pyongsan group and Junghwa group of Hwangju Formation, and minority of them are included in the sedimentary rocks of Jikhyon Formation, Mukchon Formation, and Onsong

Formation. In addition, the sedimentary metamorphic apatite deposits occurred within the rocks of Rangnim Complex, Jungsan Complex, and Hwanghae Complex. The apatite ore bodies in the carbonatite deposits are composed of apatite-calcite carbonatite within Neoproterozoic and Paleoproterozoic sedimentary metamorphic rocks. Most of industrial apatite deposits including Phungnyon, Yongyu, and Jungsan deposits belong to the category of carbonatite deposits. The apatite ore bodies are included within the carbonatite rocks which are developed in veins within the altered granites.

According to their distribution characteristics, ore bodies are subdivided into Ryusongsan, Orijae, Sansong, Tokungsan, Jangjae, and Joljol ore bodies. Among them,

Ryusongsan and Orijae ore bodies have been already tunneled and Sansong ore body has not been yet developed until now. In this paper, we focus on exploration targeting in Sansong district. The ore bodies occurred in the form of parallel veins in the study area. The veins are divided or merged along their strike and slope direction. The width and slope of the veins change at depth, and the border between ore bodies and host rocks is relatively clear. The ore types are divided into carbonatite, altered, and oxide, and they can be subdivided into some groups according to the characteristics of mineral association. Carbonatite is the main ore type in the ore bodies, and they occur in the form of phlogopite-apatite-calcite and apatite-calcite. The altered ore bodies are developed inside the host rocks in contact between carbonatite and host rocks. The composition of altered ores depends on the composition of host rock and type of alteration. In the case of biotite gneiss, the apatite ores occur in the form of apatite-calcite-biotite and apatite-quartz-feldspar-biotite. The altered ores are dominantly developed within the biotite gneiss and granitic gneiss in Sansong district. The oxide ore types are developed in the weathered zones of all the ore bodies, and they are mainly located in the southwestern part of Sansong district. The average depth of weathered zones is 10 to 20 m. The oxide ores are apatite-vermiculite and apatite-clay. The genesis of the mineral deposit in the study area had been considered to be diagenesis in the past. But recent studies showed that the mineral deposits in the study area would occur by intrusion of carbonatite magma and metasomatism of pneumatolytic hydrothermal fluid following intrusion of ultramafic–mafic magma through several stages although the main magma source has not been clarified so far and it has been in the focus of the study yet (Choe et al. 2011; Ju 2020).

Based on the consideration of ore geology in the study area (Fig. 3), we modeled carbonatite, biotite gneiss, and granitic gneiss as host rocks of apatite ore bodies. In addition, we used  $P_2O_5$  values from the borehole data in the

study area. So, there included four factors in total for 3D mineral prospectivity modeling of apatite deposits.

## Methods and results

### Three-dimensional modeling

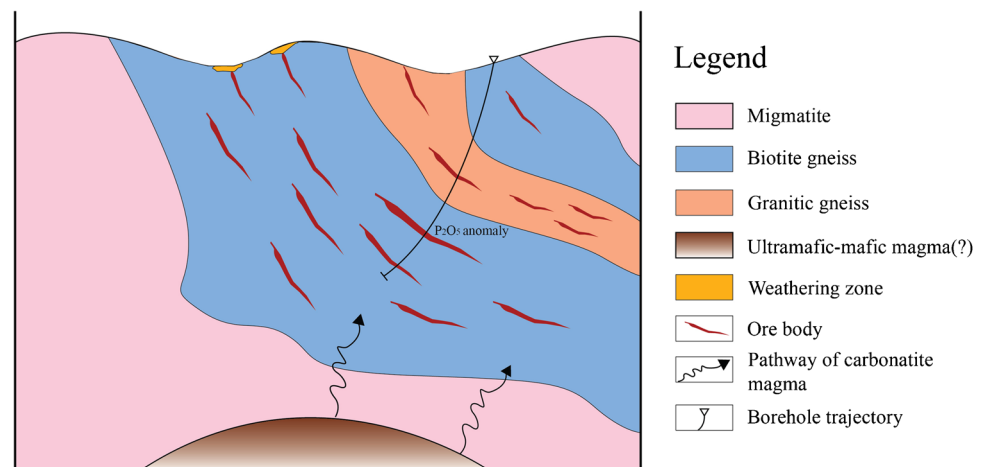
#### Building datasets

In this paper, the spatial geological datasets designed and derived for three-dimensional modeling for three-dimensional MPM in the study area can be summarized as follows: (a) the plane maps (e.g., 5000 geological map, 1:2000 deposit-scale map) with surface survey dataset; (b) the 25 mineral exploration line cross section data; and (c) the 61 mineral exploration borehole dataset with  $P_2O_5$  assay (the XYZ coordinates, assay data, borehole trajectory, lithology logging). In the mineral exploration borehole data, the number of exploration line is 25 and its spacing is 100 m. The number of boreholes is 61, and sample length is about 1 m on average with maximum of 4.1 m. The average depth of boreholes is 194.6 m with minimum of 74.25 m and maximum of 281.1 m. The trajectory data of boreholes are also added to the borehole datasets. The average inclination of boreholes is approximately  $85^\circ$  and azimuth is  $340^\circ$  in the 21 exploration lines with the number 49–59 and  $45^\circ$  in the 4 exploration lines with the number 66–69. The geological map, cross section, and borehole datasets were designed and built in ArcGIS 10.4 platform.

#### GOCAD software and SGrid

Mineralization processes occur in 3D, and they are better represented by their geological signatures in 3D datasets. Therefore, MPM would be best modeled in 3D space rather than in 2D. But regional-scale 3D MPM is rarely feasible

**Fig. 3** Mineral deposit model of Sansong district, Yongyu apatite deposit



mainly because regional-scale public-domain 3D datasets over large areas are generally not available (Xiao et al. 2015). However, deposit-scale 3D datasets for specific target areas are occasionally available and can be used for delineating further drilling targets at the deposit-scale. In addition, more commercial 3D GIS products, such as GOCAD, Surpac, and Micromine (Geovia 2015; Micromine 2015; Wang et al. 2020; Cheng 2021), became widely available, and this has led to developing 3D MPM, particularly at detailed scales (Yuan et al. 2014; Xiao et al. 2015; Mao et al. 2019; Cheng 2021; Mohammadpour et al. 2021; Deng et al. 2022). One of the main challenges in 3D MPM based on 3D GIS is to efficiently incorporate 3D predictive models within 3D GIS because most of commercial 3D GIS software does not include corresponding models, modules, and tools for 3D MPM (Li et al. 2016).

GOCAD is a software which uses discrete smooth interpolation (DSI) technique as the core interpolation algorithm (Mallet 2002). It can be used to build the surface or sub-surface element which has a triangular grid structure and can be reconstructed using ArcGIS and other GIS software (Perrouy and Lindsay 2014). The DSI equation provides a powerful and efficient numerical method for modeling the geometry and the properties of curves, surfaces, and solids. In this study, we use SGrid in GOCAD 2015 software to build 3D geological model according to the need of 3D modeling after building datasets in ArcGIS 10.4 platform. An SGrid object is a flexible, 3D grid for modeling properties, computing reservoir volumes, and creating flow simulations in GOCAD. An SGrid object can contain property values either at the centers or the corners of its cells. The dimensions of the SGrid are defined by its origin, the three axes, the number of points along each axis, and the three step vectors of each cell (Fig. 4). This object is important in reservoir geology and engineering where anisotropy plays a significant role in hydrocarbon migration and accumulation. In this case, we use SGrid as main object for modeling 3D geological objects including  $P_2O_5$  grade because grade values might be considered to be anisotropic in 3D space.

### Three-dimensional geological modeling

The three-dimensional geological models for carbonatite, biotite gneiss, and granitic gneiss in the study area were constructed using the geoscientific datasets in GOCAD software. The digitized cross section data in ArcGIS were converted into surface models using DSI algorithm in GOCAD (Fig. 5).

In order to create 3D geological model, the cross section data should be first digitized in ArcGIS. Digitizing is one of the most excellent functions of ArcGIS. The digitized cross section data can be imported as cultural data (ArcView shapefile) into GOCAD. The shapefile contains several properties: XYZ and ID. The imported cross section data will be treated as curves in GOCAD. To create surface from two curves, it is necessary to link nodes, and then, curve parts are created. Before creating curve parts, it is necessary to set some parameters such as level and part name. After creating surfaces from each two curves is finished, the first and last curves are closed by using closed curves function in GOCAD. All individual parts are merged, and triangles are smoothed and interpolated using beautify triangles function. Finally, 3D geological models are obtained by using DSI algorithm in GOCAD.

### Three-dimensional modeling $P_2O_5$ grade

In this paper, 3D modeling for  $P_2O_5$  grade in Sansong district was conducted using SGrid model in GOCAD based on borehole datasets and 3D ore body model. The borehole data were converted into ASCII format and imported to GOCAD. The statistical analysis results for the  $P_2O_5$  grade values are given in Table 1.

The main steps for 3D modeling of  $P_2O_5$  grade using SGrid in GOCAD and the methodology of our 3D prospectivity modeling are summarized in Fig. 6. Three evidential factors including carbonatite, biotite gneiss, and granitic gneiss are weighted by fuzzy scores from experts after 3D modeling in GOCAD. The  $P_2O_5$  grade is interpolated by

**Fig. 4** Graphic examples of an SGrid object and its components. **a** SGrid and its step vectors. **b** SGrid and its end points (Micromine 2015)

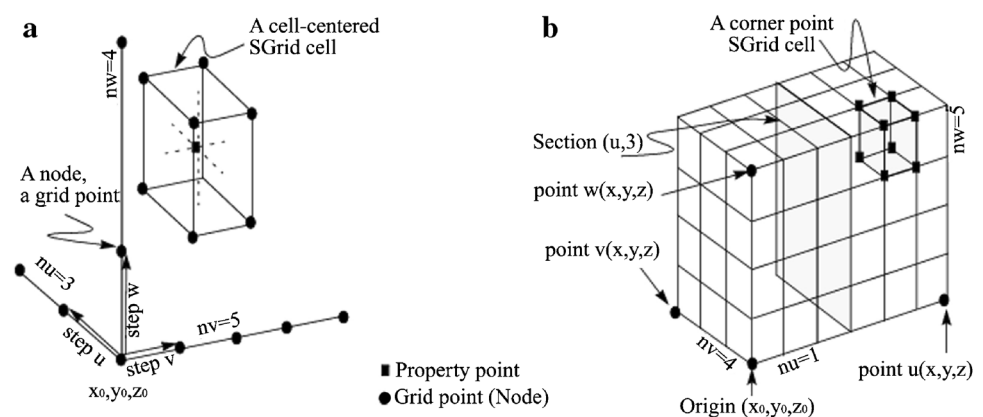


**Fig. 5** 3D geological models of **a** carbonatite, **b** biotite gneiss, and **c** granitic gneiss using DSI in GOCAD

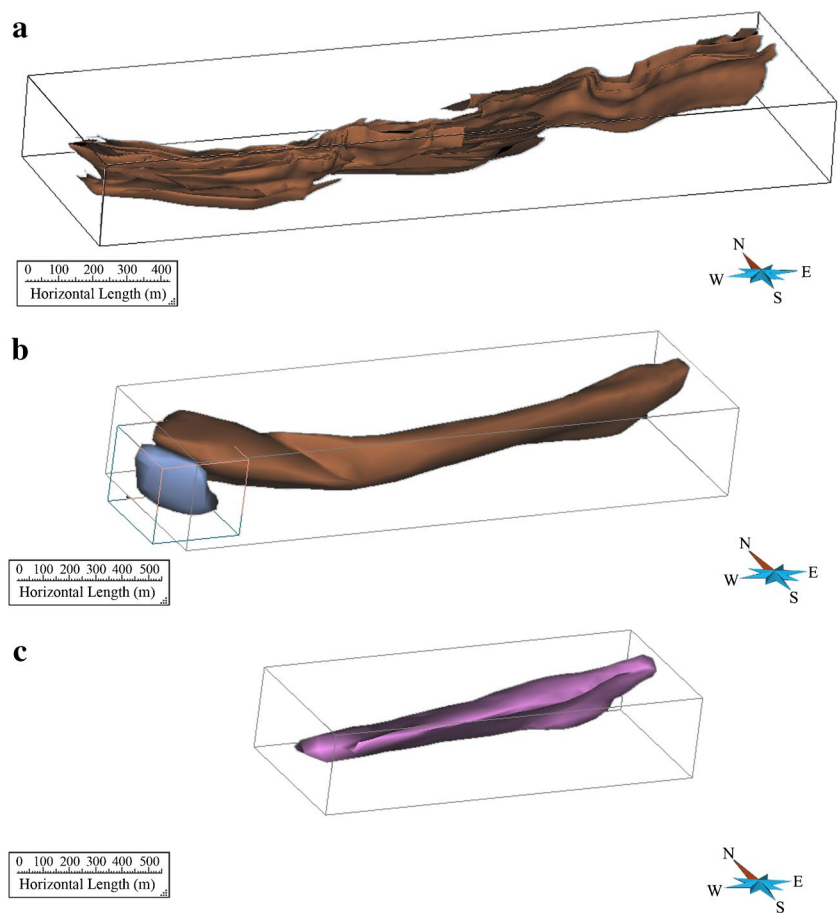


**Table 1** The statistics of  $P_2O_5$  grade values

Number of samples	Minimum (%)	Median (%)	Maximum (%)	Mean (%)	Standard deviation (%)	Variance (%)
844	0.01	6.07	17.98	6.05	2.86	8.16

ordinary kriging and weighted by continuous fuzzy membership function after 3D modeling in GOCAD. These four evidential factors are integrated by two kinds of predictive models including the fuzzy logic and the geometric average, and their results are validated by the prediction efficiency curve. Finally, the effectiveness of 3D prospectivity modeling will be compared with our previous 2D case study (Kim et al. 2019).

When creating 3D SGrid object, we used a cell size of  $100*50*25$  in 3D space in consideration of the cage of study area and computation efficiency (Fig. 7).

The ordinary kriging method was selected as an interpolation method for 3D grade modeling. For calculating an experimental variogram, the lag distance and the number of lags were assigned to 75.2 m and 30, respectively. The bandwidth and maximum number of neighborhood were assigned to  $22.5^\circ$  and 24, respectively. The three-dimensional modeling result of  $P_2O_5$  grade is given in Fig. 8.

### Three-dimensional prospectivity modeling using fuzzy logic and geometric average

Like our previous studies, we did not apply any data-driven approaches but chose fuzzy logic and geometric average belonging to a category of knowledge-driven techniques as integration methods for 3D MPM in the Sansong district. The selection of the fuzzy logic and geometric average for 3D prospectivity modeling in the study area was based on three following reasons: (1) both are relatively simple models and easy to implement in 3D MPM studies as well as in 2D MPM studies, (2) it is also to avoid the disadvantage of data-driven approaches in terms of exploration bias (Coolbaugh et al. 2007), and (3) it is to test possibility for application of the fuzzy logic and geometric average in 3D MPM for non-metal deposits. Therefore, some of borehole datasets were used to validate the predictive model results in our study.

**Fig. 6** Main steps for 3D prospectivity modeling

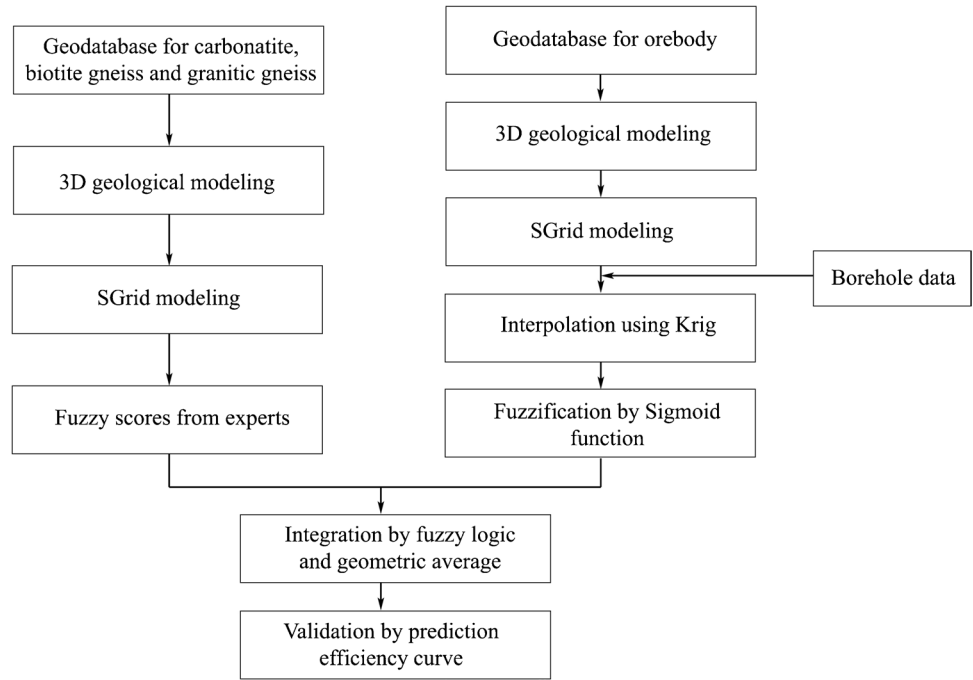


**Fig. 7** 3D SGrid object used for 3D MPM

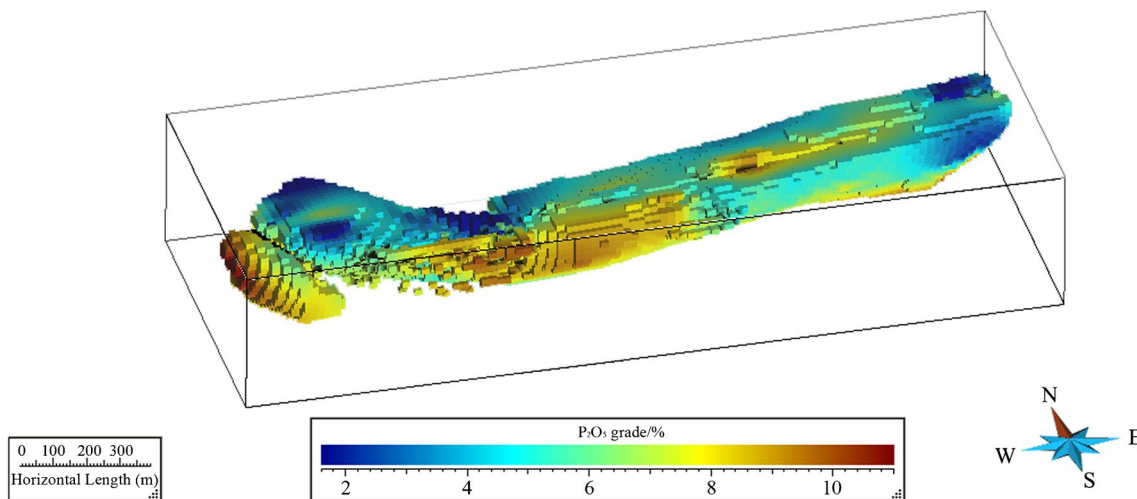
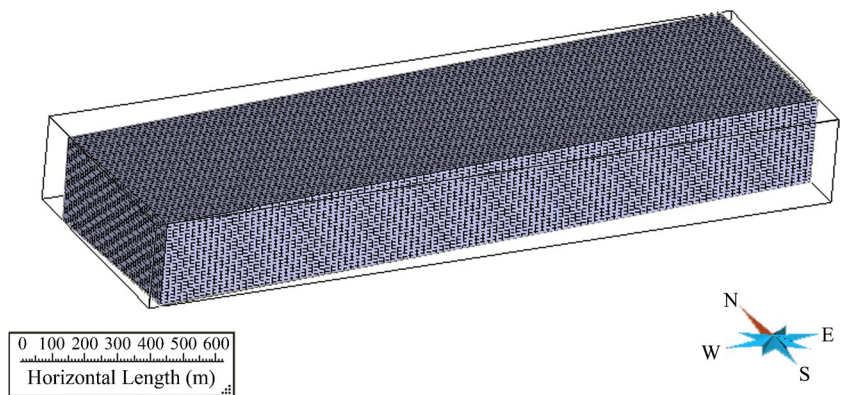


**Fig. 8** 3D modeling result of P<sub>2</sub>O<sub>5</sub> grade

### Fuzzification and integration using fuzzy logic model

The fuzzy logic model is based on fuzzy set theory, and it was first introduced by Zadeh (1965). In fuzzy set theory, the membership of a set is defined on a continuous scale from full non-membership to full membership. A fuzzy set of  $A$  is a set of ordered pairs (Nykänen et al. 2015):

$$A = \{[x, \mu A(x)] | x \in X\} \quad (1)$$

where  $X$  is a collection of objects and  $\mu A(x)$  is the membership function of  $x$  in  $A$ . The degree of membership of  $x$  in  $A$  is defined by the membership function  $\mu A(x)$ , and it can be expressed by either linear or non-linear function. Yousefi and Carranza (2015a) demonstrated that non-linear transformation is more reasonable than linear technique for fuzzification of evidential maps for MPM. Different non-linear transformation functions such as a logistic sigmoid function have been widely used for rescaling in MPM (Nykänen et al. 2015; Yousefi and Carranza 2015a, b, c). This kind of non-linear membership functions can be applied to 3D MPM studies as well as 2D study.

To rescale interpolated  $P_2O_5$  assay data, we used the following logistic sigmoid function (Yousefi and Carranza 2015a):

$$\mu(x) = \frac{1}{1 + e^{-s(x-i)}} \quad (2)$$

where  $\mu(x)$  is a fuzzy membership function;  $s$  and  $i$  are slope and inflection point of the logistic function, respectively; and  $x$  is a map value to be transformed in the  $[0, 1]$  range. Using suitable values of two parameters in Eq. (2), it is possible to transform integers and floating values of different ranges into  $[0, 1]$  values. The selection of suitable values for two parameters in Eq. (2) for calculating the fuzzy membership was conducted by trial-and-error scheme. In our case, the logistic sigmoid function expressed in Eq. (2) was applied to transform interpolated  $P_2O_5$  assay data.

For the other three evidential factors including carbonatite, biotite gneiss, and granitic gneiss, the weights for integrating with  $P_2O_5$  assay data were empirically assigned according to the importance for occurrence of apatite ore bodies because they did not have continuous voxel values. Therefore, the voxel values for these three factors are not continuous but categorical. In this study, the fuzzy scores were respectively assigned 1 for carbonatite, 0.8 for biotite gneiss, and 0.7 for granitic gneiss.

The fuzzy scores are assigned by following reasons: First, it is natural that the fuzzy score for carbonatite is 1 because it was clarified and modeled through drilling data. And ore bodies in the study area are exclusively occurred in the biotite gneiss and granitic gneiss though they are occasionally present in other country rocks. In addition, it proved that

the biotite gneiss would be slightly more favorable country rock than granitic gneiss through statistical analysis from 57 boreholes and their cross section data. It is probably because the biotite gneiss has more fractures and fissures favorable for the formation of ore bodies in the study area. Finally, these fuzzy scores are agreed with the field workers who have many experiences in this area.

In order to integrate four fuzzified evidential maps, we applied “fuzzy gamma” operators. This operator was selected because it is the compromise between the “increasing” nature of fuzzy algebraic sum and the “decreasing” effect of the fuzzy algebraic product and it is possible to adjust fine change of contribution of all evidential maps. In this study, the gamma value was assigned to 0.85 after testing many different gamma values. The 3D prospectivity map by the fuzzy logic is given in Fig. 9.

### Geometric average model

At the same time of integrating fuzzified evidential maps using fuzzy logic model, geometric average model was also applied to combine evidential maps and achieve comparative analysis.

The geometric average can be defined as the  $n$ th root of the products of values where  $n$  is the count of values. The geometric average,  $G_A$ , of a dataset  $\{v_1, v_2, \dots, v_n\}$  is written by the following (Yousefi and Carranza 2015c):

$$G_A(v_1, v_2, \dots, v_n) = \left( \prod_{i=1}^n v_i \right)^{1/n} = \sqrt[n]{v_1 v_2 \dots v_n} \quad (3)$$

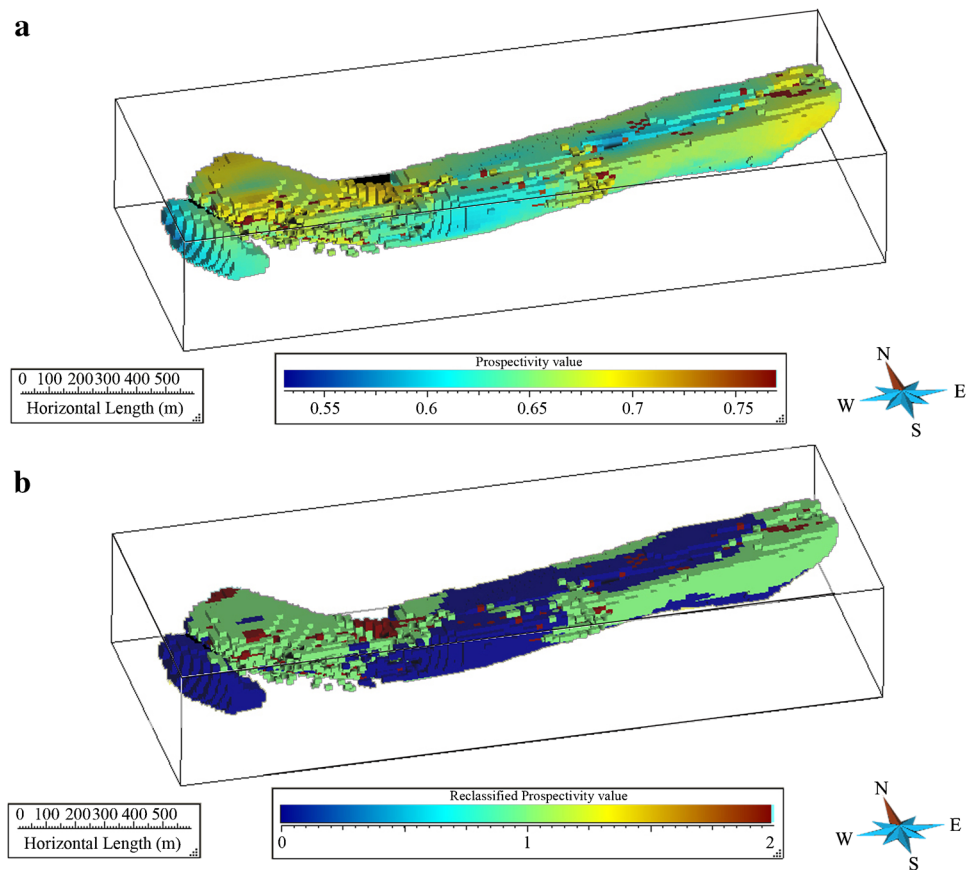
The geometric average model can be applied only to evidential maps with non-negative values. In this study, the geometric average can be easily applied to all the evidential maps because they have been already transformed using non-linear fuzzy membership function. The modified geometric average function for 3D MPM of the apatite deposit,  $G_{A-apatite}$ , for a certain unit cell of the study area can be written as follows:

$$G_{A-apatite}(F_{CA}, F_{BG}, F_{GG}, F_{P_2O_5}) = \left( \prod_{i=1}^4 F_i \right)^{1/4} = \sqrt[4]{F_{CA} F_{BG} F_{GG} F_{P_2O_5}} \quad (4)$$

where  $F_{CA}$ ,  $F_{BG}$ ,  $F_{GG}$  and  $F_{P_2O_5}$  are respectively fuzzy scores of carbonatite, biotite gneiss, granitic gneiss, and interpolated  $P_2O_5$  assay data which have been already fuzzified using logistic fuzzy membership function in fuzzy logic modeling. Among the four fuzzy scores,  $F_{CA}$ ,  $F_{BG}$ ,  $F_{GG}$  assigned by expertise are categorical and  $F_{P_2O_5}$  assigned by fuzzy membership function is continuous. Another prospectivity map for the apatite mineralization of the study area was created by using Eq. (4) (Fig. 10).



**Fig. 9** **a** 3D prospectivity modeling results by the fuzzy logic and **b** its classified results



The integration of these evidence layers using fuzzy logic and geometric average models was performed using spatial analyses in ArcGIS and script in GOCAD.

### Validation and results

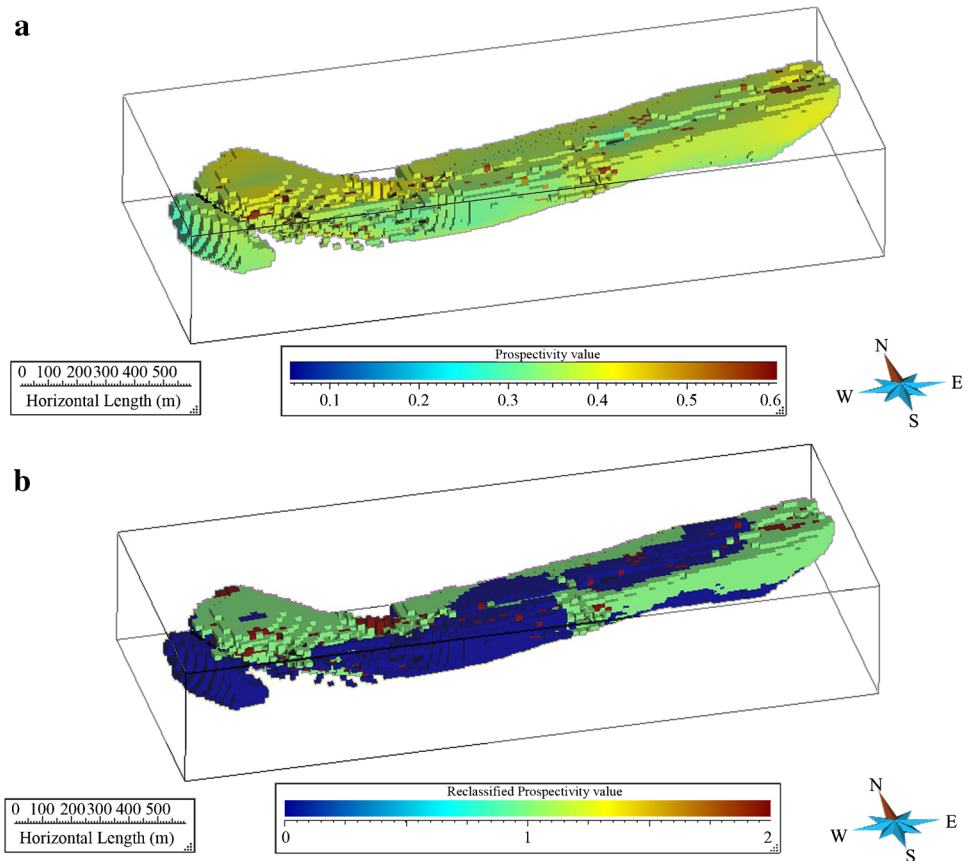
Prediction efficiency curves (or capture efficiency curves) were used to evaluate the performance of the two models. Prediction efficiency curves depict the cumulative proportion of validation data captured by a prospectivity model in cumulative proportions of the study area. Prediction efficiency curve can be plotted by the proportion of the validation data (known deposits) versus proportion of volume (or area in 2D). Prediction efficiency curve of the best prospectivity model shows an inverted “L”-shaped curve with the elbow close to (0, 1); that is, it predicts all validation data in a very small proportion of the study area, indicating a perfect prediction performance. On the other hand, an inefficient prospectivity model returns a diagonal line across the graph, that is, the proportion of the study area, indicating a random classification of prospectivity. Clearly, the higher the curve above the diagonal line, the better the performance of the prospectivity model. In order to validate the predictive models, we randomly chose 46 borehole data which had  $P_2O_5$  values more than 10% and the validation data occupies

about 5.5% of total borehole samples. In the current study, both fuzzy logic and geometric average models yield prediction efficiency curves that are above diagonal line; however, the geometric average curve lies above the fuzzy logic curve, indicating that the former performs better in predicting the validation data (Fig. 11). In this study, prediction efficiency curves were made in MATLAB R2015a.

Prediction efficiency curves can also be used to reclassify the prospectivity volumes into two or more classes. High prospectivity volumes are characterized by portions of the prediction efficiency curve that have steep slopes. They represent large portions of prospectivity volumes in relatively small proportions of the study area. On the other hand, medium and low prospectivity volumes are characterized by portions of the prediction efficiency curve that have respectively gentle and nearly horizontal slopes in relatively large proportions of the study area. The slope changing points in the prediction efficiency curves can be used as cutoff values for reclassifying into high-, medium-, and low-prospectivity zones. According to this procedure, we used the inflection points on the curves as threshold values for reclassification of the continuous-scale prospectivity results into three classes (Figs. 9 and 10).

High-prospectivity zones on the two prospectivity maps occupy 13.4% and 12.3% of the total volume occupied by

**Fig. 10** **a** 3D prospectivity modeling results by the geometric and **b** its classified results



the Sansong ore body, respectively; however, the geometric average performs better in predicting validation data (Table 2). The fuzzy logic and geometric average models capture 71.7% and 76.1% of the validation data in the high-prospectivity zones, respectively.

The better performance of the geometric average model is further illustrated by the prediction efficiency curves

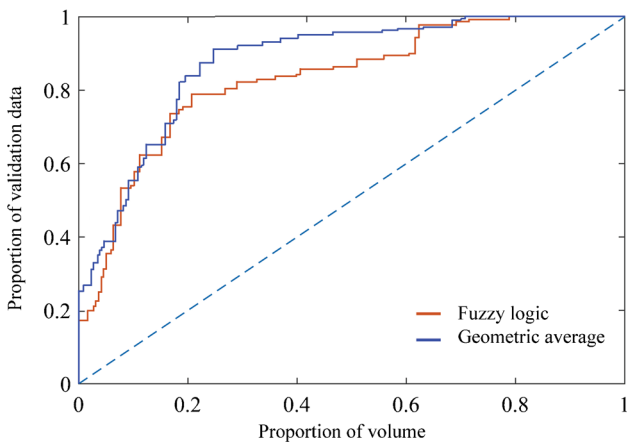


**Fig. 11** Prediction efficiency curves for fuzzy logic and geometric average models

(Fig. 11), which are conceptually similar to the capture efficiency curves but depict the performance of prospectivity models in predicting validation data. Figure 11 shows that the curve for the geometric average model lies above the curve for the fuzzy logic model in high-prospectivity areas.

The target volumes classified by the fuzzy logic occupy 13.4% of the study area and contain 71.7% of the total number of validation data. It also means that 33 out of 46 voxels for validation data are present in the most favorable volume with high prospectivity values. Meanwhile, the resulting volumes by the geometric average model occupy 12.3% of the total volume for the study area but contain 76.1% of the total volume for the validation data. In other words, 35 out of 46 total voxels are present in the most favorable volume with high prospectivity values.

### Discussion

In the current study, our focus was on answering the question “Can we use the fuzzy logic and geometric average methods for 3D mineral prospectivity modeling of non-metal resources rather than 2D MPM of metal resources in the DPR Korea?”. The answer was positive, and it can be effectively done by using 3D modeling based on SGrid model in

**Table 2** Summarized results of prospectivity modeling

Model	Zone	% volume	Validation data	
			Number	Percent
Fuzzy logic	High-prospectivity zone	13.4	33	71.7
	Medium-prospectivity zone	34.3	11	24.0
	Low-prospectivity zone	52.3	2	4.3
Geometric average	High-prospectivity zone	12.3	35	76.1
	Medium-prospectivity zone	36.4	10	21.7
	Low-prospectivity zone	51.3	1	2.2

GOCAD. In other words, extension of 2D MPM towards 3D MPM was easily implemented by introducing SGrid model in GOCAD.

In our study, both fuzzy logic and geometric average models yield prediction efficiency curves that are above diagonal line, and it indicates that both results are definitely better than a result based on a random selection of target volumes, and two models are useful for 3D MPM in Sansong district, Yongyu apatite deposit, DPR Korea. In addition, the geometric average curve lies above the fuzzy logic curve, and it indicates that the former performs better in predicting the validation data like 2D case study. We compared the results with those in our previous 2D case study (Kim et al. 2019). In our previous 2D study, the target areas classified by the fuzzy logic occupy 15% of the whole study area and contain 78% of the total number of validation data. In the current 3D study, they are 15% and 71.7%, respectively. Meanwhile, in the 2D study, the resulting areas by the geometric average model occupy 13% of the study area but contain 93% of the total number of known mineral occurrences. The numbers are 12.3% and 76.1% in the current 3D study, respectively. Even though the target areas or volumes classified by the fuzzy logic and the geometric average are almost the same in 2D and 3D case studies, the areas with high prospectivity values in 2D contain slightly more validation data than the volumes with high prospectivity values in 3D. The comparison results indicate that prediction results in 3D are slightly less effective than those in 2D study, but two models can be also applied to 3D studies as well as 2D. The main advantages of the fuzzy logic and geometric average methods are that they can be easily and simultaneously applied to 3D MPM without any additional troublesome extensions as well as 2D MPM, and they can be used for discrete-scale evidential maps as well as continuous-scale evidential maps.

In the modeling results, the most favorable districts which give the highest prospectivity values both in fuzzy logic and geometric average are mainly consistent from each other, and they are considered to be new drilling targets, and they can also be valuable for the design of future mining and development. The most of favorable voxels are mainly distributed in biotite gneiss and granitic gneiss, and it is because the mineralization of apatite had predominantly occurred in those two layers. In addition, higher prospectivity values of biotite

gneiss show that it would have more fractures and fissures favorable for the formation of apatite compared with granitic gneiss and others. Meanwhile, some high prospectivity voxels are distributed in the zones with low values of  $P_2O_5$  grade, and it is mainly because they are included within the carbonatite zone with highest fuzzy scores.

The study area is elongated from the west to the east and short from the north and the south. The current mining and production of ore bodies are being implemented in Manpung and Phungnyon districts, the eastern parts 2.5 km distant from Sansong district, Yongyu apatite deposit. The current districts have been already drilled over 800 m at depth, and they will be exhausted after some years, and we need to prepare some new districts for future mining and production. The Sansong district may be the only choice for future mining and production in the Yongyu apatite deposit. According to our results, the westmost, central, and northeast parts of the study area can be regarded as the most unfavorable zones, and the west and southeast parts are considered to be the most favorable zones with highest prospectivity values. Therefore, the most favorable target areas can be divided into two parts: west and southeast. However, the depth of prospectivity volumes is different from zones. The west part with high prospectivity values is distributed from the surface to 250 m at depth, and it is relatively widespread. Meanwhile, the southeast part is located from the top to 350 m at depth, and it is relatively deep and narrowly distributed from the top to the depth. The volume of the former is slightly larger than the latter, and the condition of the former for drilling and production is much more convenient than the latter. Our research results were presented for the geological survey of Yongyu mine to design more detailed geological survey and to drill some additional boreholes.

Some kinds of uncertainty must be involved in our 3D prospectivity modeling, and they should be discussed here. The main sources of uncertainty in mineral prospectivity modeling are related to some factors, and they can be classified into two categories of uncertainties: stochastic and systemic uncertainties (Lisitsin et al. 2014; Zuo et al. 2015). Stochastic uncertainty is mainly associated with data quality, and systemic uncertainty is related to modeling procedures. In our study, systemic uncertainty can be represented by assigning fuzzy scores reflecting expert opinion through statistical study of cross section data.

The uncertainty linked to 3D modeling could not be significant though it would not be quantified because 3D model was created through stochastic mathematical modeling (DSI) in GOCAD based on hard data (borehole data). For the  $P_2O_5$  grade, the geometric average as well as fuzzy logic can assign continuous weights and avoid the problem of uncertainty due to simplification and discretization of continuous value spatial evidences into some classes using intervals.

## Conclusions

In this paper, two knowledge-driven methods using the fuzzy logic and geometric average were simultaneously applied to generate 3D mineral prospectivity models in Sansong district, Yongyu apatite deposit, DPR Korea. GIS and GOCAD modeling techniques based on two knowledge-driven approaches can provide a fast and economic way to separate 3D prospectivity target areas for apatite deposit in the study area although they have some subjective elements because of using expert opinions just as 2D case.

The spatial evidences for 3D MPM modeling consisted of four geological layers, and three evidences were weighted by experts. And  $P_2O_5$  assay data were transformed into the [0, 1] range by using the logistic sigmoid function. The three categorical fuzzy scores and one continuous fuzzy score were integrated by the fuzzy logic and geometric average models. The fuzzy logic and geometric average methods can use the same fuzzification methodology based on the same fuzzification scheme; therefore, it is very economic and efficient to simultaneously apply two predictive models for 3D MPM. In addition, they can be easily applied to 3D case simply by converting pixels into voxels as well as 2D MPM.

The geometric average modeling performs better than the fuzzy logic modeling in predicting the validation data although the results are slightly worse than those in 2D. The comparative analysis result demonstrated that most of the validation voxels are distributed in volumes with high prospectivity values. The target volumes classified by the fuzzy logic occupy 13.4% of the total volume and contain 71.7% of the total number of validation voxels. Compared with the fuzzy logic, the resulting voxels by the geometric average occupy 12.3% of the total volume but contain 76.1% of the total number of the validation voxels.

The prediction efficiency analysis shows that the curve for the geometric average model lies above the curve for the fuzzy logic model. The locations of validation data in Sansong district were randomly selected among borehole data.

To summarize our study, the fuzzy logic and geometric average can be effectively used for 3D non-metallic MPM study as well as 2D metallic MPM. Our future work will focus on continuous fuzzification of spatial evidences based on reasonable and objective approach instead of subjective

opinions and 3D metallic MPM case studies using more spatial evidences based on sophisticated modelings.

## Concluding remarks

The main findings of this study are as follows:

1. In this paper, two knowledge-driven methods using the fuzzy logic and geometric average were simultaneously applied to generate 3D prospectivity target volumes in the study area. Two predictive models used the same fuzzification strategy of evidential maps, and they exhibited good generalization capability in 3D MPM.
2. The results were validated by the prediction efficiency curves indicating the curve for the geometric average model lied above the curve for the fuzzy logic model.
3. The most favorable target areas can be divided into two parts: west and southeast. The west part with high prospectivity values is distributed from the surface to 250 m at depth, and it is relatively widespread. Meanwhile, the southeast part is located from the top to 350 m at depth, and it is relatively deep and narrowly distributed from the top to the depth.

**Acknowledgements** The authors thank the geological survey of Yongyu mine for their contributions to provide geological data of Yongyu apatite deposit and their support during the field work. We also appreciate Prof. Abdullah M. Al-Amri, Editor-in-Chief; Prof. Biswajeet Pradhan, Chief Editor and Associate Editor; and three anonymous reviewers for their thorough reviews of the manuscript and their constructive comments which helped us to improve this paper.

## Declarations

**Conflict of interest** The authors declare no competing interests.

## References

- Behera S, Panigrahi MK (2021) Gold prospectivity mapping in the Sonakhan Greenstone Belt, Central India: a knowledge-driven guide for target delineation in a region of low exploration maturity. *Nat Resour Res* 30:4009–4045
- Chen YL, Wu W, Zhao QY (2020) A bat algorithm-based data-driven model for mineral prospectivity mapping. *Nat Resour Res* 29:247–265
- Cheng J (2021) Construction and visualization of a three-dimensional model of an engineering geological body. *Arabian J Geosci*. <https://doi.org/10.1007/s12517-021-06600-x>
- Choe P, Ho D, Yun J, Sin Y, Jo S (2011) Encyclopedia of Korean Geology, Vol. 8. Industrial Publishing House, p 536
- Coolbaugh MF, Raines GL, Zehner RE (2007) Assessment of exploration bias in data-driven predictive models and the estimation of undiscovered resources. *Nat Resour Res* 16:199–207
- Deng H, Zheng Y, Chen J, Yu SY, Xiao KY, Mao XC (2022) Learning 3D mineral prospectivity from 3D geological models using convolutional neural networks: application to a structure-controlled

- hydrothermal gold deposit. *Comput Geosci*. <https://doi.org/10.1016/j.cageo.2022.105074>
- Ford A, Miller JM, Mol AG (2015) A comparative analysis of weights of evidence, evidential belief functions, and fuzzy logic for mineral potential mapping using incomplete data at the scale of investigation. *Nat Resour Res*. <https://doi.org/10.1007/s11053-015-9263-2>
- Geovia (2015) GEOVIA SurpacTM-geology and mine planning software. The 3D EXPERIENCE Company, Vancouver. <http://www.geovia.com/products/Surpac>
- Hosseini SA, Abedi M (2015) Data envelopment analysis: a knowledge-driven method for mineral prospectivity mapping. *Comput Geosci* 82:111–119
- Ju JK (2020) The geological and economic geological characteristics of carbonatites in DPR Korea. PhD thesis. Kim Chaek University of Technology, p 231
- Khosravi V, Shirazi A, Shirazy A, Hezarkhani A, Pour AB (2022) Hybrid fuzzy-analytic hierarchy process (Ahp) model for porphyry copper prospecting in Simorgh area, eastern Lut block of Iran. *Mining* 2:1–12
- Kim YH, Choe KU, Ri RK (2019) Application of fuzzy logic and geometric average: a Cu sulfide deposits potential mapping case study from Kapsan basin, DPR Korea. *Ore Geol Rev* 107:239–247
- Kreuzer O, Miller A, Peters K et al (2015) Comparing prospectivity modelling results and past exploration data: a case study of porphyry Cu-Au mineral systems in the Macquarie Arc, Lachlan Fold Belt, New South Wales. *Ore Geol Rev* 71:516–544
- Li RX, Wang GW, Carranza EJM (2016) GeoCube: a 3D mineral resources quantitative prediction and assessment system. *Ore Geol Rev* 89:161–173
- Li TF, Xia QL, Zhao MY, Gui Z, Leng S (2020) Prospectivity mapping for tungsten polymetallic mineral resources, Nanling Metallogenic Belt, South China: use of random forest algorithm from a perspective of data imbalance. *Nat Resour Res* 29:203–227
- Li H, Li XH, Yuan F, Jowitt SM, Dou FF, Zhang MM, Li XL, Li Y, Lan XY, Lu SM, Ding WX (2022) Knowledge-driven based three-dimensional prospectivity modeling of Fe-Cu skarn deposits; a case study of the Fanchang volcanic basin, anhui province, Eastern China. *Ore Geol Rev*. <https://doi.org/10.1016/j.oregeorev.2022.105065>
- Lisitsin VA, Porwal A, McCuaig TC (2014) Probabilistic fuzzy logic modeling: quantifying uncertainty of mineral prospectivity models using Monte Carlo simulations. *Math Geosci* 46:747–769
- Liu JT, Cheng QM (2019) A modified weights-of-evidence method for mineral potential prediction based on structural equation modeling. *Nat Resour Res* 28(3):1037–1053. <https://doi.org/10.1007/s11053-018-9435-y>
- Mallet JL (2002) *Geomodeling*. Applied Geostatistics Oxford University Press, New York, pp 1–10
- Mao XC, Ren J, Liu ZK, Chen J, Tang L, Deng H, Bayless RC, Yang B, Wang MJ, Liu CM (2019) Three-dimensional prospectivity modeling of the Jiaojia-type gold deposit, Jiaodong Peninsula, Eastern China: a case study of the Dayingezhuang deposit. *J Geochem Explor* 203:27–44
- Micromine (2015) *Micromine exploration & 3D mine design software*. Micromine Pty Ltd., Perth. <http://www.micromine.com/products-downloads/micromine>. Accessed 25 Nov 2015
- Mohammadpour M, Bahrroudi A, Abedi M (2021) Three dimensional mineral prospectivity modeling by evidential belief functions, a case study from Kahang porphyry Cu deposit. *J African Earth Sci*. <https://doi.org/10.1016/j.jafrearsci.2020.104098>
- Nykänen V, Lahti I, Niiranen T, Korhonen K (2015) Receiver operating characteristics (ROC) as validation tool for prospectivity models-amagmatic Ni-Cu case study from the Central Lapland Greenstone Belt, Northern Finland. *Ore Geol Rev* 71:853–860
- Paek R, Kang H, Jon G, Kim Y, Kim Y (1993) *Geology of Korea*. Foreign Languages Books Publishing House, p 619
- Perrouy S, Lindsay MD (2014) 3D modeling of the Ashanti Belt, southwest Ghana: evidence for a litho-stratigraphic control on gold occurrences within the Birimian Sefwi Group. *Ore Geol Rev* 63:252–264
- Prado EMG, Roberto C, Carranza EJM, Motta JG (2020) Modeling of Cu-Au prospectivity in the Carajás mineral province (Brazil) through machine learning: dealing with imbalanced training data. *Ore Geol Rev*. <https://doi.org/10.1016/j.oregeorev.2020.103611>
- Ren M, Chen J, Shao K, Zhang S (2016) Metallogenic information extraction and quantitative prediction process of sea floor massive sulfide resources in the Southwest Indian Ocean. *Ore Geol Rev* 76:108–121
- Shabani A, Ziaii M, Monfared MS, Shirazy A, Shirazi A (2022) Multi-dimensional data fusion for mineral prospectivity mapping (MPM) using fuzzy-AHP decision-making method, Kodegan-Basiran region, East Iran. *Minerals*. <https://doi.org/10.3390/min12121629>
- Shirazi A, Hezarkhani A, Pour AB, Shirazy A, Hashim M (2022) Neuro-fuzzy-AHP (NFAHP) technique for copper exploration using advanced spaceborne thermal emission and reflection radiometer (ASTER) and geological datasets in the Sahlabad mining area, East Iran. *Remote Sens*. <https://doi.org/10.3390/rs14215562>
- Shirazy A, Ziaii M, Hezarkhani A (2021) Geochemical behavior investigation based on K-means and artificial neural network prediction for titanium and zinc, Kivi region. *Iran Bull Tomsk Polytech Univ* 332:113–125
- Tao JT, Yuan F, Zhang NN, Chang JY (2021) Three-dimensional prospectivity modeling of Honghai volcanogenic massive sulfide Cu-Zn deposit, Eastern Tianshan, Northwestern China using weights of evidence and fuzzy logic. *Math Geosci* 53:131–162
- Wang Y, Chen JP, Jia DH (2020) Three-dimensional mineral potential mapping for reducing multiplicity and uncertainty: Kaerqueka polymetallic deposit, Qinghai province, China. *Nat Resour Res* 29:365–393
- Xiao K, Li N, Porwal A, Holden E, Bagas L, Lu Y (2015) GIS-based 3D prospectivity mapping: a case study of Jiama copper-polymetallic deposit in Tibet, China. *Ore Geol Rev* 71:357–367
- Xiong YH, Zuo RG (2018) GIS-based rare events logistic regression for mineral prospectivity mapping. *Comput Geosci* 111:18–25
- Yousefi M, Carranza EJM (2015a) Fuzzification of continuous-value spatial evidence for mineral prospectivity mapping. *Comput Geosci* 74:97–109
- Yousefi M, Carranza EJM (2015b) Prediction-area (P-A) plot and C-A fractal analysis to classify and evaluate evidential maps for mineral prospectivity modeling. *Comput Geosci* 79:69–81
- Yousefi M, Carranza EJM (2015c) Geometric average of spatial evidence data layers: a GIS-based multi-criteria decision-making approach to mineral prospectivity mapping. *Comput Geosci* 83:72–79
- Yuan F, Li X, Zhang M, Jowitt SM, Jia C, Zheng T, Zhou T (2014) Three-dimensional weights of evidence-based prospectivity modelling: a case study of the Baixiangshan mining area, Ningwu Basin, Middle and Lower Yangtze Metallogenic Belt, China. *J Geochem Explor* 145:82–97
- Zadeh LA (1965) *Fuzzy sets* 8. Institute of Electric and Electronic Engineering, Information and Control, pp 338–353
- Zhang H, Xiao JY, Carranza EJM, Yang F (2019) Maximum entropy and random forest modeling of mineral potential: analysis of gold prospectivity in the Hezuo-Meiwu district, West Qinling Orogen, China. *Nat Resour Res* 28:645–664. <https://doi.org/10.1007/s11053-018-9425-0>
- Zuo R, Zhang Z, Zhang D, Carranza EJM, Wang H (2015) Evaluation of uncertainty in mineral prospectivity mapping due to missing evidence: a case study with skarn-type Fe deposits in Southwestern Fujian Province, China. *Ore Geol Rev* 71:502–515

Springer Nature or its licensor (e.g. a society or other partner) holds exclusive rights to this article under a publishing agreement with the author(s) or other rightsholder(s); author self-archiving of the accepted manuscript version of this article is solely governed by the terms of such publishing agreement and applicable law.